PNAS
www.pnas.org

# Supplementary Information for

## The bright side of PV production in snow-covered mountains

**Annelen Kahl, Jerome Dujardin, Michael Lehning**

**Annelen Kahl.**
**E-mail: annelen.kahl@epfl.ch**

**This PDF file includes:**





www.pnas.org/cgi/doi/10.1073/pnas.1720808115

## Supporting Information Text

### Data availability

In order to provide transparancy and the possibility for others to either reproduce our results or to develope our methods further, we have made all non-confidential data sets as well as all our code with documentation available on the Envidat Data Platform, doi:10.16904/envidat.47. The current version is the orinigal code use for this paper, but we will soon publish a second version that is more versitile and easier to use. Data from SwissGrid and MeteoSwiss cannot be openly distributed but can be made available for research upon request.

### PV production calculated with the SUNWELL model (detailed)

The electricity production of any PV panel is determined by the shortwave radiation that vertically impinges onto the panel surface. Other factors such as age of the panel, ambient temperature and panel technology further affect the panel efficiency, but in this study, we use standard values, since the focus is on input variability and not on panel efficiency. The solar input, i.e. plane of array (POA) irradiance can be accurately modeled and varies by far the most with time and space compared to all other factors. The two basic inputs are: Global Surface Incoming Shortwave radiation (SIS) and Direct Incoming Shortwave radiation (SISDIR). The former indicates how much energy reaches a unit horizontal surface in total. It is the sum of direct beam radiation which reaches the earth's surface on a straight trajectory from the sun and of diffuse radiation which has been scattered on its pathway through the earth's atmosphere. Since the ratio of beam and diffuse radiation varies throughout the day and with the presence of clouds, we use SISDIR to compute the diffuse component. Both, SIS and SISDIR are derived from METEOSAT satellite imagery and were provided by MeteoSwiss at hourly resolution on a 1.25 degree minute grid (1). Over Switzerland this roughly corresponds to a pixel size of 1.6 km in East-West direction and 2.3 km in North-South direction. The products used in this study were computed using the Heliomont algorithm (2) which is specifically conceived for mountainous terrain and includes a snow-cloud discrimination that avoids the misqualification of snow cover as clouds, which would lead to an underestimation of surface irradiance and has been shown to bias irradiance estimates (3, 4). More details of the data acquisition and post-processing are described by Stoeckli (2). Quality assessments of this product are presented below in the section 'Evaluation of the SIS radiation product from Meteosat imagery' .

Figure S1 visualizes the modeling steps to compute the POA irradiance from incoming shortwave radiation and the installation geometry of the PV panel. After the separation of global into direct and diffuse radiation, we use the isotropic sky model developed by Liu and Jordan (5) given in Equation 1 to transpose each of the components onto the panel surface. For the transposition of the direct beam radiation $I_b$, the angle between instantaneous beam and panel normal needs to be calculated for every time step, as it changes throughout the day and throughout the year. This angle determines the ratio $R_b$ of beam irradiance on the tilted surface to the irradiance on the horizontal surface. Panel azimuth determines at which time of the day maximum beam radiation is collected. Depending on the tilt, this effect will be more or less pronounced. The closer the panel is to a horizontal position, the smaller the effect of the azimuth angle. The tilt also decides at which time of the year the panel is most productive. Steeper tilts elevate production in winter, while shallower angles give preference to summer production. Diffuse radiation $I_d$, reaches the panel from the portion of the sky that is within the panel's hemisphere. Hence the steeper the panel tilt $\beta$ is from the horizontal, the smaller the portion of the sky that contributes to the panel's diffuse radiation budget. The isotropic sky model for the diffuse radiation assumes that all directions contribute the same amount of diffuse radiation. The last component of POA irradiance is the radiation that is reflected from the ground. Again, we assume an isotropic model for simplicity, although Painter et al. and Odermatt et al. have shown that anisotropy of snow reflectance increases with grain size, sun zenith angle, wavelength and snow wetness (6, 7). Like the diffuse radiation, this portion depends on the amount of ground that is within the panel's hemisphere and thus is a function of its tilt $\beta$. The estimatation of ground reflection $\rho_g$ is described in more detail in the following section. The sum of the three contributions, beam direct, diffuse and ground reflected yield the plane of array shortwave radiation:

$$POA = I_b R_b + I_d \left( \frac{1 + \cos\beta}{2} \right) + I \rho_g \left( \frac{1 - \cos\beta}{2} \right) \quad [1]$$

We convert POA into electricity production assuming a constant system efficiency of 15%.

### Ground reflected shortwave radiation

The amount of radiation that is reflected back from the ground is a function of the surface albedo, which varies between different land surface cover types. Water, wet soil and forests reflect between 5%-15% of the incoming radiation, while fresh snow can reach values as high as 95%. To account for this large discrepancy and the variation throughout the year, we use the Meteosat-derived albedo product MSG.ALB. It provides hourly albedo values, which sets it apart from many other albedo products that are commonly available at daily resolution. Due to its high temporal resolution it can account for the significant change in albedo due to evolving solar zenith angle throughout the day. MSG.ALB provides the all-pixel albedo and not the albedo of the snow-covered portion of the pixel. Since we cannot predict where in the pixel the snow is present and whether it is within the view shed of the PV panel, it seems more prudent to work with the lower albedo value of the mixed pixel. However, with expert knowledge of local professionals, one could envision placing PV panels in a location with a ground reflectance that

is higher than the pixel-wide average value. In order to visualize a simplified representation of temporal and spatial presence of snow cover we compute the snow cover duration (SCD) in number of days for each pixel. A day is classified as snow day if the pixel albedo given by the MSG.ALB product is 0.4 or higher. SCD is a commonly used parameter to characterize the presence of snow and it has been calculated previously by Huesler et al. (8) for the entire Alps. Their analysis was based on AVHRR imagery and yields matching trends for the mountains of Switzerland.

## Evaluation of the SIS radiation product from Meteosat imagery

The HelioMont product has been validated against five different ground measurement networks (2) and three ground measurement stations (3). The largest errors in diffuse and direct radiation on shorter time scales were found on summer cloud-free days during the central hours of the day and were associated to the use of monthly climatological means for areosol characteristics and water vapor column (instantaneous locally measured values yield far superior results). The evaluation of monthly average values shows that the seasonal cycle of all radiation components is well reproduced. In Davos for example (one of the evaluation sites for our model and a typical alpine site with complex terrain) a mean average bias of $12W/m^2$, was found. To compliment the findings from literature we conducted a small evaluation study ourselves to have a closer look at seasonal variations in accuracy of the SIS product. For the years 2014-2016 we compared daily total irradiance values from two station of the Alpine Surface Radiation Budget (ASRB) network (9) with the daily values of the corresponding satellite pixels. The evaluation sites are located at Weisfluhjoch (WFJ, 2693m) and in the town of Davos (SLF, 1560m). The statistics in Table S1 show good agreement at annual scale: total irradiance is underestimated by only 4% and 1% for SLF and WFJ respectively. When we look at the temporal development of this underestimation throughout time (Figure S2), we can see clear seasonal trends. The difference ASRB - SIS is highest in spring and fall and smaller or reversed in summer and winter. Especially at Weisfluhjoch positive and negative deviations almost compensate each other throughout the year, as represented by the small mean difference, but relatively high RMSD. For our study we can assume simultaneous deviations of modeled from actual electricity production.

## Topographic shading effects in the radiation product

Obstruction of solar irradiance can significantly lower the productivity of a PV panel and needs to be taken into account when selecting the installation site. In flat, urban areas the major concerns are surrounding buildings, which vary over very small scales and cannot be accounted for in our model. We have to assume that any individual PV owner would consider this prior to installation. In the mountains the surrounding terrain can cast large shadows that might decrease the time of direct solar irradiance by several hours. This is particularly true lower down in the valleys and during the winter months. The HelioMont algorithm that calculates the irradiance product used in this paper accounts for terrain shading through the use of a digital elevation model (DEM) (10). For each pixel, 100 horizon angles of the surrounding terrain are calculated over a radius of 25km. That corresponds to an azimuthal sector of 3.6 degrees between individual horizons. For any instance of the sun falling below the local horizon, the pixel's direct beam irradiance is set to zero. More details about the DEM and the associated calculations of terrain shading are given in (2) (section 8.6, 9.2 and 9.4)

## Maximum allowed cover fraction for PV installations

Table S2 lists the different maximum cover fractions that we impose for various landsurface cover types throughout Switzerland. They represent a best guess as to how much PV can realistically be placed in the respective types of land. Urban and industrial land receive the highest percentage, since we count all south oriented roofs to be potential installation zones in addition to public places, gardens and housefronts. As panel tilt increases, the foot print of the installed panels decreases drastically until vertical panels simply represent a line on the ground, with all the surface area stacked in the vertical dimension. At this point we have not undertaken a detailed GIS study to assess whether all the selected pixels are accessible by road, but the Alps and especially Switzerland has a well-developed road network reaching high elevations and due to the large amount of hydropower installations, even grid connections are often already in place. We would also like to remind the reader that this paper does not measure up to an exhaustive development plan for PV installations in Switzerland, rather we want to introduce a new approach toward the seasonal energy gap and provide information about the available potential and physical constraints; It is our hope to trigger the interest of researchers from different backgrounds, such that subsequent studies can shine light on the many questions that remain unanswered here.

## Simplifications in our estimate of electricity production

In view of our study's objective – analyzing the relative spatial variability of PV production in different geographic regions – we decided to lump together all contributions to the overall system efficiency and work with one universal, constant efficiency of 15%. This entails the following assumptions (and our respective justifications):

1. Constant panel DC efficiency - Assuming spatial and temporal invariance of panel efficiency will likely result in an underestimate of production in cold regions and during winter months (11, 12). Hence, we are putting the urban scenario at an advantage with respect to the mountain scenario.
2. Constant reflection characteristics of the panel surface and their independence of tilt angle - This effect is indenpendent of geolocation, it depends on material properties and might change or be completely eliminated in the future, hence we do not consider any variability.

3. Constant AC/DC converter efficiency - The efficiency associated to all electric components that treat the panel's DC output varies highly between different systems and also depends on their connection to the grid. The associated loss can be up to 30%, but newest maximum power point tracking (MPPT) algorithms can reach an efficiency of up to 99%. Assuming that all potential new installations can reach the same level of performance, we keep it constant. 4. Neglecting degradation of panel performance due to age - this factor is independent of location and will systematically develop at any installation (13)
5. Constant loss due to soiling by dirt, dust, pollen and other particles that cover the PV panel - Compared dry and sandy areas this effect is relatively weak in the mid-latitudes of the northern hemisphere ((14), Figure 2). Urban and industrial areas in particular tend to have a higher rate of soiling than high-elevation mountainous regions. It has further been found that accumulation of snow and its sliding off the panel has a better cleaning effect than rain and that steeper panel tilts thus decrease the loss due to soiling (15). Again, accounting for this would improve modeled performance of installations at high elevations and steep tilt angles compared to the urban roof-top installations. Many models that account for the technical details above have been developed (16) (17) and more refined calculations for the transposition from incoming global radiation to panel normal shortwave radiation have been proposed (18). Furthermore, the selection of online PV estimation tools has grown over the past years. A good overview is given by (19).

## Evaluation of electricity production estimates

To show that our modeled electricity production captures the temporal behavior of actual production throughout the year we conducted an evaluation study with four different PV installations in Switzerland. Table S3 shows the characteristics of the individual installations.

Our method to estimate PV production is conceived to compare the electricity production of a generic panel in various different locations, and we assume the same overall system efficiency everywhere. Consequently, the model is not set up to account for the individual system characteristics of specific panel types. As mentioned in the conclusions and in the 'limitations of our model' section, there are several other aspects that lower the initial DC output efficiency of the PV panel. And indeed, we see a consistent overestimation when we model production based on the factory-assigned panel efficiencies of the PV panels used in this evaluation. To better capture the overall system efficiency of the different installations, we multiply the DC output efficiency with the ratio of measured to modeled annual total production. Overall, the comparison in Figure S3 shows a good agreement between measured and modeled behavior. The production profiles of the vertical installations with their characteristic double peak in spring and fall stand in clear contrast to the production profiles of the shallow installations, which have one large peak in summer. Below the seasonal scale, short term variations are also quite closely captured by SUNWELL. In addition to the modeled production that was calculated from satellite-derived products (blue lines), we also show modeled production where the SIS time series of global incoming shortwave radiation was substituted with measured values of surface incoming global radiation from the exact location of the PV installlations (9), available for Weisfluhjoch and Davos. These latter results, depicted in green, allow us to estimate how much of the difference between modeled and measured electricity production is due to an error in the satellite product and how much of it is due to the combined errors from the transposition of surface-incoming to panel-normal radiation and the consecutive conversion to electricity. The green line lies almost exclusively between the measured and modeled timeseries, splitting the difference in production into a small error contribution from the satellite product and a larger contribution from the remaining model steps. Furthermore, we can observe a small but persistent overestimation of production during the winter months. The fact that this difference is more expressed for the two shallow PV installations at Laret and Lac des Toules suggests temporary accumulation of snow on the panels as possible cause. In the smoothed times series it looks as if this is a continuous difference throughout the winter, but when we compare the two time series at daily resolution it becomes apparent that the differences occur only very punctually. A second period of overestimation during the summer months at SLF and WFJ can most likely be attributed to high temperatures on those vertically facades that temporarily decreased the efficiency of the panel.
Those last two effects illustrate the shortcomings of our simplified model, as listed in the previous paragraph, and indicate a clear direction to future improvements.

## References


1. Dürr B, Zelenka A (2009) Deriving surface global irradiance over the Alpine region from METEOSAT Second Generation data by supplementing the HELIOSAT method. *International Journal of Remote Sensing* 30(September 2013):5821–5841.
2. Stoeckli R (2017) The HelioMont surface solar radiation processing 2017 update. *Scientific Report MeteoSwiss* (93):122 pp.
3. Castelli M, et al. (2014) The HelioMont method for assessing solar irradiance over complex terrain: Validation and improvements. *Remote Sensing of Environment* 152:603–613.
4. Dürr B, Zelenka A, Mueller R, Philipona R (2010) Verification of CM-SAF and MeteoSwiss satellite based retrievals of surface shortwave irradiance over the Alpine region. *International Journal of Remote Sensing* 31(15):4179–4198.
5. Liu BYH, Jordan RC (1963) A Rational Procedure for Predicting The Long-Term Average Performance of Flat-Plate Solar-Energy Collectors. *Solar Energy* 7(2):53–74.
6. Odermatt D, et al. (2005) Seasonal study of directional reflectance properties of snow. *EARSeL eProceedings 4* (2):203–214.
7. Painter TH, Dozier J (2004) Measurements of the hemispherical-directional reflectance of snow at fine spectral and angular resolution. *Journal of Geophysical Research Atmospheres* 109(18):1–21.
8. Hüsler F, Jonas T, Riffler M, Musial JP, Wunderle S (2014) A satellite-based snow cover climatology (1985-2011) for the European Alps derived from AVHRR data. *Cryosphere* 8(1):73–90.

9. Philipona R, Marty C (2001) *Surface Radiation Budget and Cloud Forcing Over the Alps* ed. von Bremen L. (A. Deepak Pub, Hampton, Va.).
10. Farr T, Kobrick M (2007) The shuttle radar topography mission. *Rev. Geophys.* 45:1–133.
11. Sze SM, Kwok KN (1981) *Physics of Semiconductor Devices.* (John Wiley & Sons, New York), p. 832.
12. Singh P, Singh SN, Lal M, Husain M (2008) Temperature dependence of I-V characteristics and performance parameters of silicon solar cell. *Solar Energy Materials and Solar Cells* 92(12):1611–1616.
13. Jordan D, Kurtz S, VanSant K, Newmiller J (2016) Compendium of photovoltaic degradation rates. *Progress in photovoltaics* 24:978–989.
14. Maghami MR, et al. (2016) Power loss due to soiling on solar panel: A review. *Renewable and Sustainable Energy Reviews* 59:1307–1316.
15. Afridi MA, et al. (2017) Determining the Effect of Soiling and Dirt Particles at Various Tilt Angles of Photovoltaic Modules To cite this version :. *International Journal of Engineering Works* 4(8):143–146.
16. Huld T, et al. (2011) A power-rating model for crystalline silicon PV modules. *Solar Energy Materials and Solar Cells* 95(12):3359–3369.
17. Sukamongkol Y, Chungpaibulpatana S, Ongsakul W (2002) A simulation model for predicting the performance of a solar photovoltaic system with alternating current loads. *Renewable Energy* 27(2):237–258.
18. Perez R, Stewart R, Arbogast C, Seals R, Scott J (1986) An anisotropic hourly diffuse radiation model for sloping surfaces: Description, performance validation, site dependency evaluation. *Solar Energy* 36(6):481–497.
19. Suri M, et al. (2008) First Steps in the Cross-Comparison of Solar Resource Spatial Products in Europe in *Eurosun 2008.*
20. Steinmeier C (2013) CORINE Land Cover 2000/2006 Switzerland. Final Report, (Federal Office for the Environment (FOEN)), Technical report.

**Table S1. Statistics of comparison between SIS and ASRB at Weisfluhjoch (2693m) and Davos (1560m)**

| | Davos | Weisfluhjoch |
|---|---|---|
| RMSD [$W/m^2$] | 25.4 | 32.9 |
| mean Diff [$W/m^2$] | 1.2 | 6.6 |
| 3-year mean ratio of annual total production SIS/ASRB | 0.96 | 0.99 |

**Table S2. Maximum allowance of installed PV surface for different land surface cover types [% of pixel surface]; Source of land surface cover types: Swiss Federal Statistical Office (20).**

| Surface Cover Type | Maximum Coverage |
|---|---|
| Urban area | 5% |
| Industrial area | 5% |
| Mine, dump, construction | 0% |
| Artificial, non-agricultural vegetation | 3% |
| Arable land | 3% |
| Permanent crops | 3% |
| Pastures | 3% |
| Heterogeneous agricultural areas | 3% |
| Forests | 0% |
| Scrub/herbaceous vegetation | 4% |
| Open spaces | 5% |
| Wetlands and lakes | 0% |

**Table S3. Panel characteristics for the PV installations used to evaluate the production modeled in this paper.**

| Location | Weisfluhjoch | Davos | Laret | Lac des Toules |
|---|---|---|---|---|
| Abreviation | WFJ | SLF | LRT | LDT |
| Lat/Lon | 46.83/9.81 | 46.81/9.85 | 46.84/9.87 | 45.92/7.20 |
| Elevation [m] | 2693 | 1560 | 1510 | 1810 |
| Tilt [°] | 90 | 90 | 35 | 30 |
| Aspect | south | south | south | south |
| Area [$m^2$] | 70 | 124 | 78 | 1.63 |
| DC efficiency [%] | 15 | 19.3 | 15.9 | 15.9 |

**Table S4. Required surface area [$km^2$] of installed PV for urban and mountain scenarios displayed in Figure 5 and Figure 6.**

| | 2011 | 2012 | 2013 | 2014 | 2015 | 2016 |
|---|---|---|---|---|---|---|
| Urban (40° tilt) | 53 | 55.9 | 60.4 | 57.8 | 54.3 | 59.5 |
| Mountain (90° tilt) | 54.5 | 54.9 | 54.1 | 59 | 54.4 | 54.9 |
| OR: Mountain (65° tilt) | 45.6 | 46.2 | 46.2 | 50 | 45.8 | 46.4 |

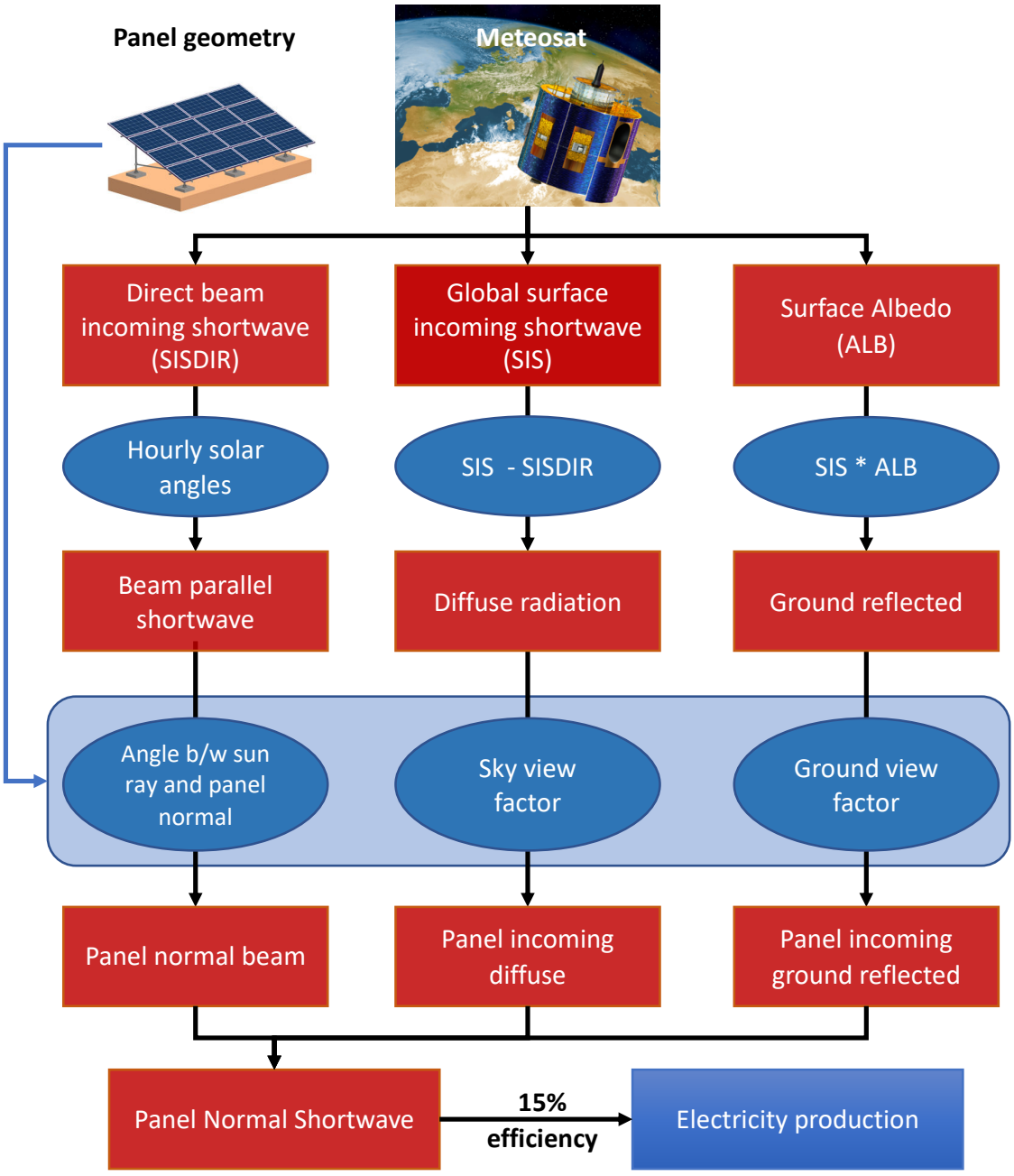


**Fig. S1. SUNWELL modeling steps from satellite-derived irradiance to electricity production.** The calculation is based on three data sets (provided to us by Meteoswiss) that are derived from satellite imagery captured with the SIVIRI instruments on Meteosat Second Generation satellites: Global (SIS) and direct (SISDIR) incoming shortwave radiation (onto a horizontal surface), as well as broadband surface albedo (ALB) at hourly resolution; The resulting electricity production is specific for the panel's geolocation and geometry (tilt and aspect angle).

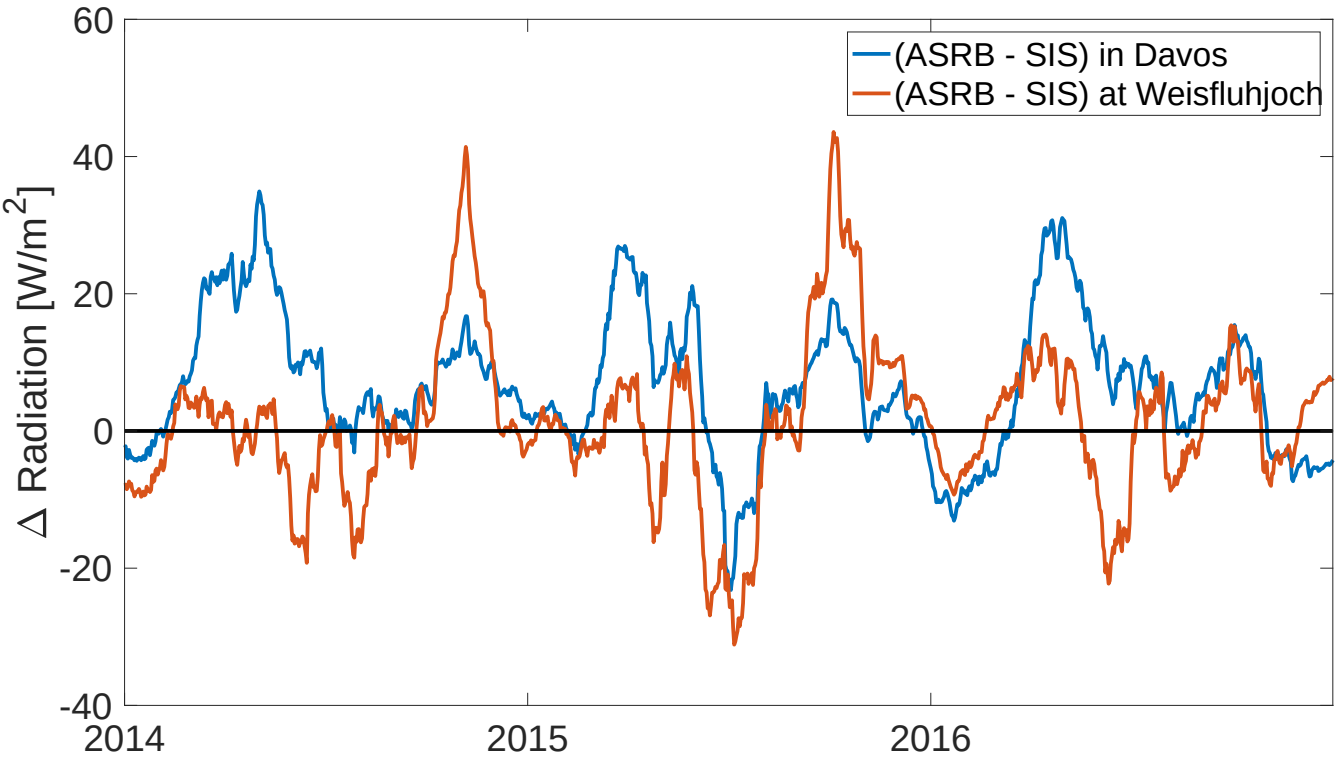


**Fig. S2. Difference between radiation values from ground-measured ASRB and from satellite-derived SIS at two alpine sites**; Weisfluhjoch (2693m) and Davos (1560m). Blue line: ASRB - SIS in Davos. Red line: ASRB - SIS at Weisfluhjoch.

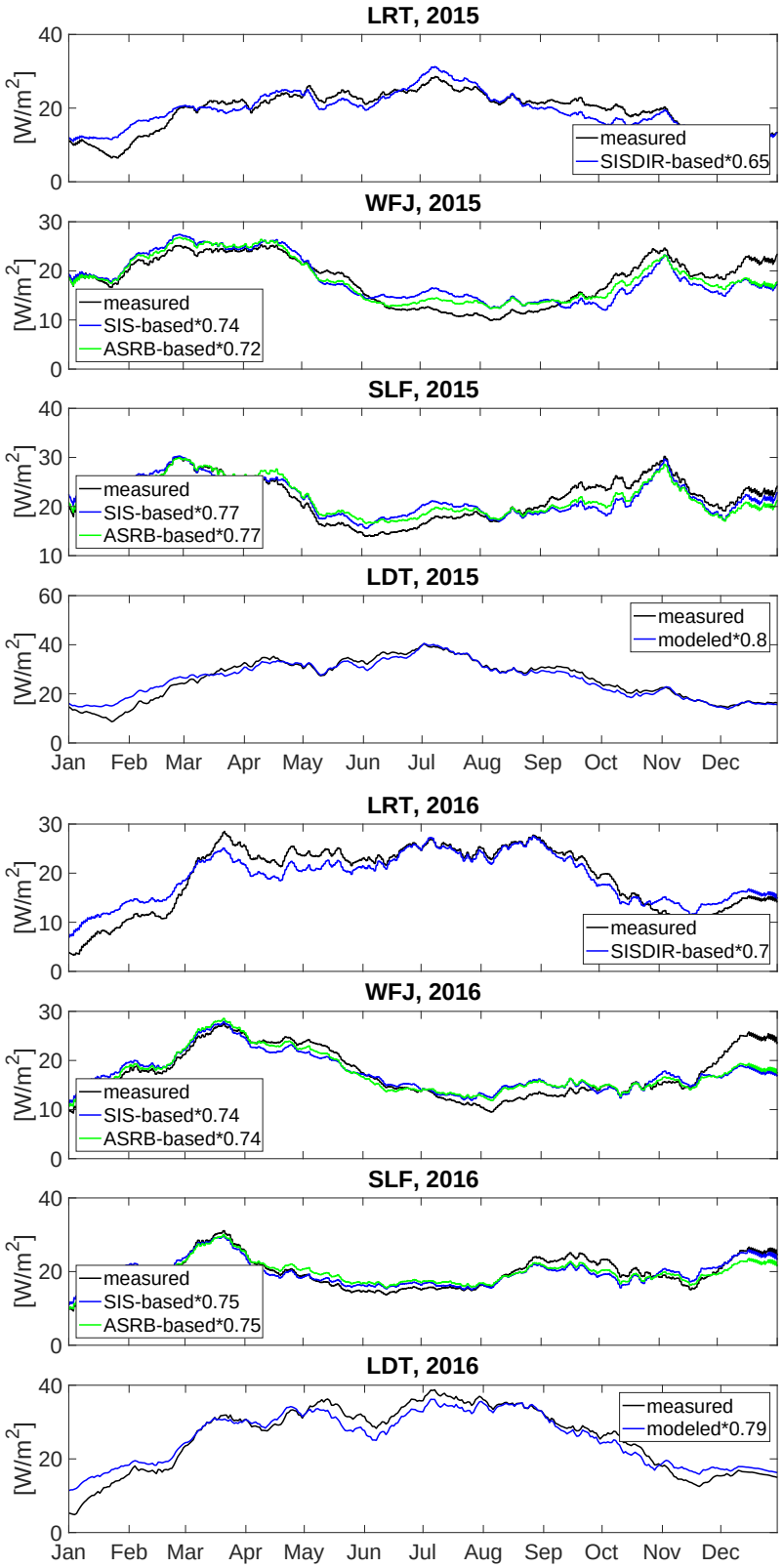


**Fig. S3. Comparison of measured and modeled PV production** at several locations in Switzerland for the years 2015/2016. For specification of the PV installations see Table S3.

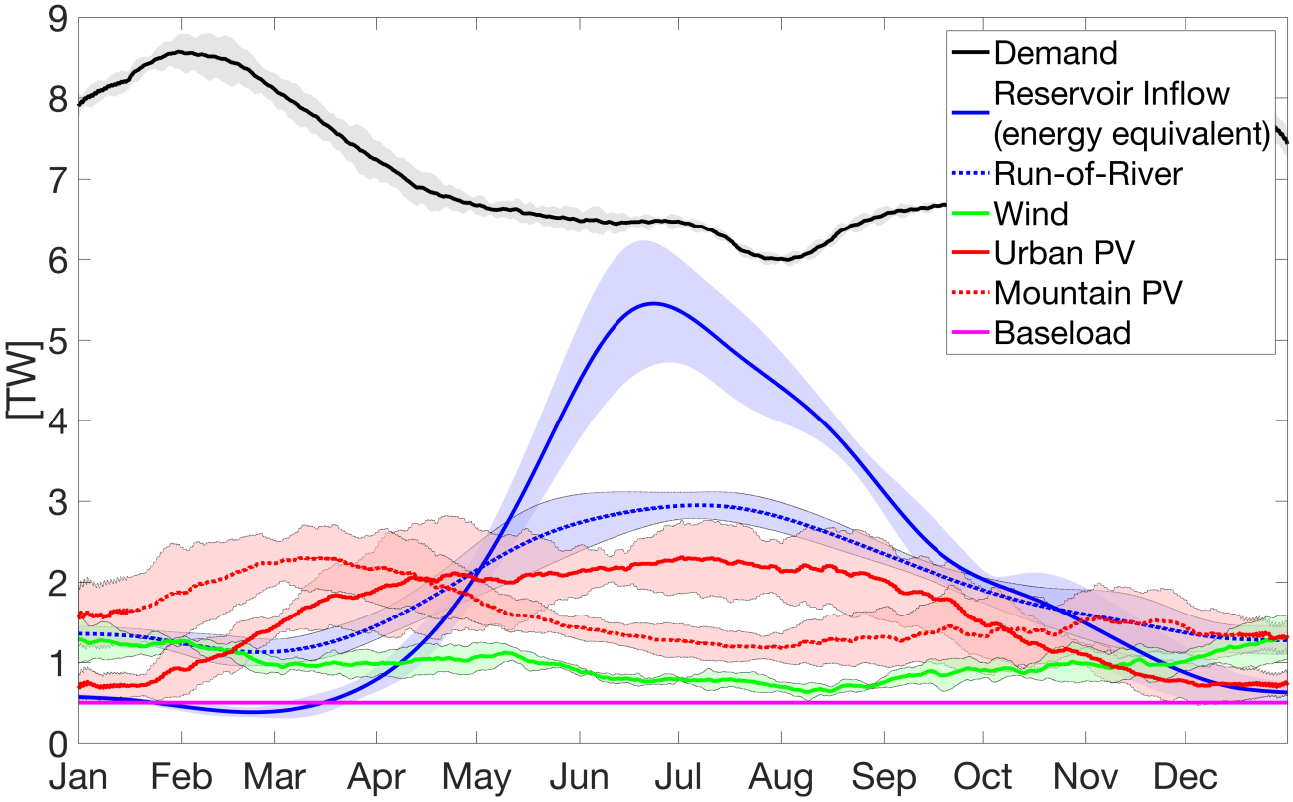


**Fig. S4. Annual profile of demand and generation in a fully renewable Switzerland.** Time series of 6-year average (2011-2016) of demand (black) and all generating sources (lines) with standard deviation (shaded area). Smoothed using 30-day moving mean filter.